BEAM DYNAMICS IN SLC[1]

Ralph W. Assmann
Stanford Linear Accelerator Center, Stanford University, Stanford CA 94309

Abstract

Beam dynamics issues affect many different aspects of the SLC performance. This paper concentrates on the multi-particle beam dynamics in the linac and the associated limitations that are imposed on the overall SLC performance. The beam behavior in the presence of strong wakefields has been studied in order identify ways to optimize the performance and to predict the expected emittances in high performance linacs. Emittance measurements and simulations are presented for the SLAC linac and are compared in detail. As the overall SLC performance depends on the accelerator stability, the tuning stability is discussed. Results are shown and the consequences for the performance of the SLC are discussed.

1 INTRODUCTION

The Stanford Linear Collider (SLC), the world's first linear collider, is now in its eighth year of operation. The SLC delivers e^+e^- collisions at a center-of-mass energy of 91.2 GeV and explores the Z-resonance. It provides the unique opportunity to experimentally explore the beam dynamics that is relevant to high performance linear colliders. Limitations can be assessed, theoretical and numerical models can be checked and possible optimization schemes can be tested. There are many crucial ingredients to the understanding and successful operation of a linear collider. This paper concentrates on the beam dynamics in the SLAC linac.

The 30 years old SLAC linac, upgraded for SLC, has a length of 3 km and accelerates electron and positron beams from an initial beam energy of 1.19 GeV to about 47 GeV. The accelerating gradient of the S-Band (2.856 GHz) structures is about 17 MeV/m. In the ideal case the normalized transverse beam emittances $\gamma\varepsilon_x$ and $\gamma\varepsilon_y$ are conserved during acceleration. However, unavoidable imperfections in connection with dipole mode wakefields can cause large emittance dilutions. An increase in the transverse beam emittances directly limits the achievable luminosity L:

$$L = f_{rep} \cdot \frac{N_e^2}{4\pi \sqrt{\varepsilon_x \varepsilon_y} \sqrt{\beta_x^* \beta_y^*}} \qquad (1)$$

Beam disruption is neglected here. The repetition rate f_{rep}, the β-functions β_x^* and β_y^* at the interaction point and the beam current N_e are to a large extent determined by the machine design. The magnitude of the transverse emittances, however, are largely determined by imperfections in the linac. The understanding of the multi-particle beam dynamics in the SLAC linac is crucial in order to minimize the emittance dilutions, to achieve maximum tuning stability and to optimize the integrated luminosity.

2 WAKEFIELDS IN THE SLAC LINAC

In the SLAC linac high current bunches (about 6 nC or $3.5\ 10^{10}$ particles) are accelerated to 47 GeV. The particles induce dipole wakefields in the RF structures, causing subsequent beam deflections. In the easiest case a single bunch is described by two particles ("head" and "tail"), each carrying half the bunch charge. As the head particle enters off-center into the structure it excites a transverse dipole wakefield that causes a deflection of the tail particle. The tail beam ellipse is offset with respect to the head beam ellipse and the projected emittance is increased. The principle of wakefield generated emittance dilution is illustrated in Figure 1.

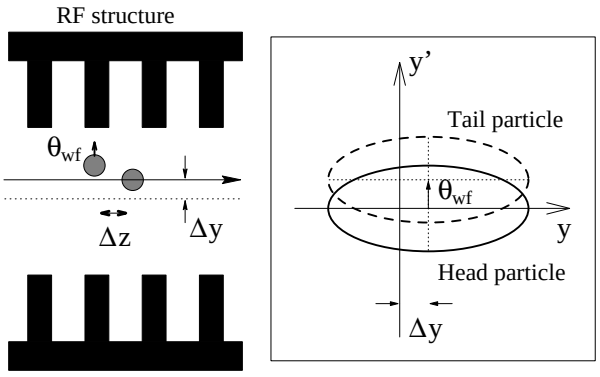

Figure 1 Principle of a wakefield generated increase in the projected emittance. A single bunch is represented by two particles. The projected beam emittance is increased due to a wakefield kick θ_{WF}.

The calculated wakefield functions in the SLAC linac are shown in Figure 2 as a function of distance Δz (e.g. between head and tail particle). The transverse wakefield deflection θ_{WF} in a structure with length L_{struc} is obtained from the transverse wakefield function W_{transv}:

$$\theta_{WF} = W_{transv}(\Delta z) \cdot \frac{e Q_1 L_{struc}}{E_2} \cdot \Delta y_1 \qquad (2)$$

Two slices, a leading slice "1" and a trailing slice "2" are considered. Slice "1" excites the wakefield with its charge

[1] Work supported by the Department of Energy, contract DE-AC03-76SF00515.

Q_1 and its offset Δy_1. Taking into account the distance Δz between the slices and the energy E_2 of slice "2", the deflection angle is obtained. Wakefield deflections θ_{WF} are always induced if the beam does not travel through the centers of all accelerating structures. The important measure for wakefield generated emittance dilution is therefore the RMS structure misalignment with respect to the beam.

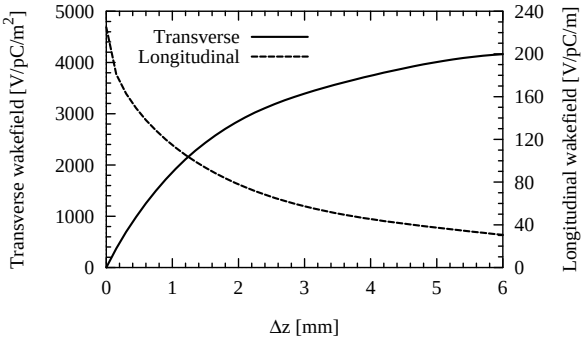

Figure 2 Calculated transverse and longitudinal wakefield functions for the SLC [1].

Modeling

The behavior of intense beams in the presence of strong wakefields and multiple interacting imperfections can be described accurately with numerical computer programs. The simulations for this paper were done with the new "LIAR" program [2]. This program allows to calculate chromatic, dispersive and wakefield generated emittance dilutions in a misaligned linac. Table 1 summarizes the default parameters that were used for the SLAC linac simulations.

Linac optics	Split-tune lattice [3] (July 1996)
Bunch population	$3.5\ 10^{10}$
Longitudinal bunch shape	42 MV compressor voltage (measured) [4]
Initial $\gamma\varepsilon_x$ / $\gamma\varepsilon_y$	30 / 3.5 mm-mrad
Quadrupole misalignment	100 μm (rms x, y)
BPM to quad misalignment	100 μm (rms x, y)
Structure misalignment (12 m girders)	200 μm (rms x, y)

Table 1 Default parameters for the linac simulations.

BNS damping

In addition to emittance dilutions, transverse wakefields can cause beam-breakup. In a two particle model, the wakefield deflections induced from the oscillating head particle defocus the tail particle until it falls behind 90º in betatron phase advance. Travelling 90º behind the oscillating head particle, wakefield deflections then add up resonantly and the tail is driven to higher and higher oscillation amplitudes.

This resonant beam-breakup can be avoided if so-called "BNS-damping" is implemented. Using the slope of the accelerating RF, an energy difference is between head and tail is induced ("correlated energy spread"). With a proper choice of RF phases, the defocusing wakefield effects for the tail can then be cancelled by chromatic effects from the quadrupoles. Ideally, the normalized amplitude of a betatron oscillation is one along the whole linac (same trajectories of head and tail).

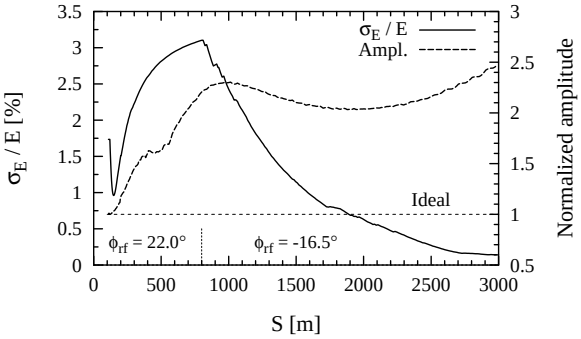

Figure 3 Simulated energy spread and normalized amplitude of a betatron oscillation along the SLAC linac.

Figure 3 illustrates the BNS setup that was used in the SLAC linac during the 1996 run. The beam was located at RF phases of +22º and -16.5º, leading to a 5% reduction in available beam acceleration. Several boundary conditions limit the efficiency of BNS that can be achieved in the SLAC linac:

1. There is no efficient BNS energy spread in the beginning of the linac.
2. The energy spread must be reduced to 0.15% at the end of the linac in order to meet the Final Focus chromatic bandwidth.
3. The RF phases must not become to large. Enough beam acceleration must be maintained in order to accelerate the beams to 46.6 GeV.

The efficiency of BNS in the SLAC linac is illustrated in Figure 3 with the normalized amplitude of a betatron oscillation. It grows by a factor of 2.5, indicating only partial BNS damping. For SLC, BNS is limited by the available beam acceleration in the linac. Note, that a stronger lattice would allow to implement better BNS damping. For a comparison of the measured and simulated normalized amplitude see [5].

3 EMITTANCE TRANSPORT

The principle of wakefield generated growth in the projected emittance was illustrated in Figure 1. If the trajectories are steered flat (minimizing the BPM readings) the residual emittance growth in the SLAC linac is unacceptably large. This is illustrated in Figure 4 for the vertical plane. The normalized emittance is simulated to grow by about 27 mm-mrad in x and 21 mm-mrad in y. With-

out wakefields, dispersion dilutes the emittance by 5.1 mm-mrad in x and 3.9 mm-mrad in y. Emittance growth is clearly dominated by wakefields.

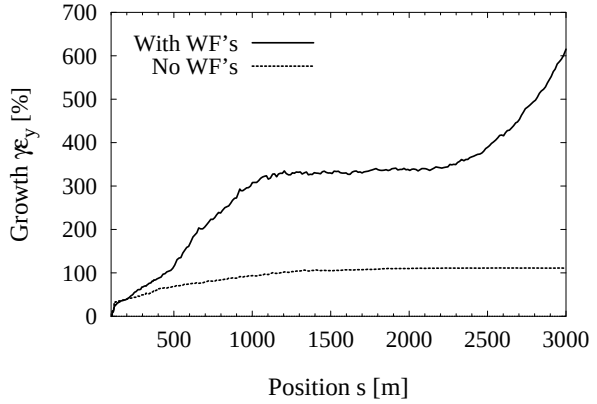

Figure 4 Simulated average vertical emittance along the linac for flat trajectories, with and without wakefields.

In 1991 so called "oscillation bumps" were introduced to optimize the emittances [6]. Betatron oscillations are generated along the linac in order to induce head-to-tail deflections that cancel the existing wakefield "banana"-shape of the linac bunch. A theoretical description is given in [2].

Typically two bumps are used parasitically during SLC operation in order to empirically minimize the measured emittances in sector 11 and sector 28 of the linac (the linac is divided into 30 sectors). The two bumps represent 16 degrees of freedom (2 x 2 phases x 2 planes x 2 beams). As an emittance measurement takes several minutes, emittance tuning requires typically several hours. Figure 5 shows a measured horizontal trajectory after emittance optimization.

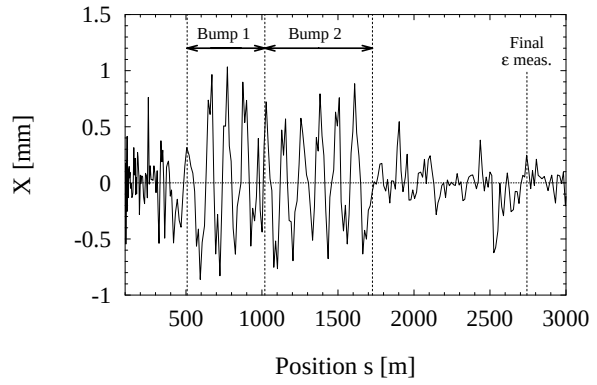

Figure 5 Horizontal linac trajectory with bumps during record luminosity on June 21st.

The simulated average vertical emittance growth after bump optimization is shown in Figure 6. The normalized emittance is reduced to the level expected from the linac dispersion at the locations of the emittance measurements. The bumps work well and compensate essentially all wakefield effects. The emittance after optimization is limited by dispersion which also is reduced somewhat by the bumps. Note that the emittance in Figure 6 grows rapidly in the end of the linac. Wakefield effects are uncompensated after the emittance measurement near the end of the linac. This growth is reduced through the use of synchrotron light screens just before the arcs at 3000 m..

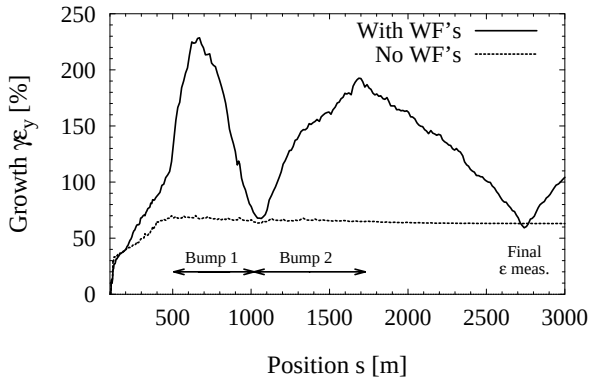

Figure 6 Simulated average vertical emittance along the linac after bump optimization.

Emittance performance in 1996

The linac beam emittances are measured regularly during the SLC operation. Every two hours the measurements are saved into a database that tracks the history of important accelerator and beam parameters. The database values for emittance measurements were analyzed for the 1996 SLC run.

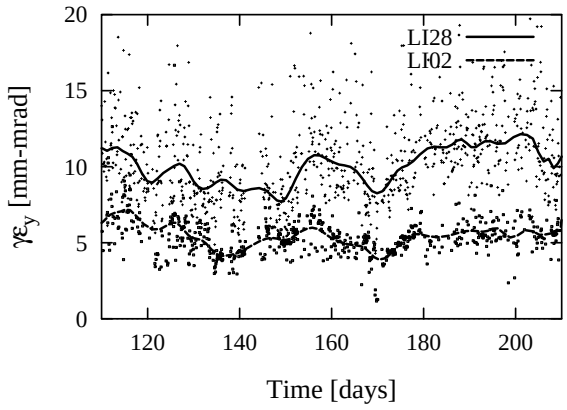

Figure 7 Measured vertical emittances against time for the beginning (LI)2) and end (LI28) of the SLAC linac. The data covers the period from April 1st to July 31st.

The vertical electron emittances in the beginning and end of the SLAC linac are shown in Figure 7. In order to summarize the 1996 emittance performance, the emittance measurements at the end of the linac were analyzed as a function of the incoming emittance. The results are shown in Figure 8 where they are compared to simulation results. Emittance measurements were filtered in order to

eliminate flyers outside of two standard deviations around the average.

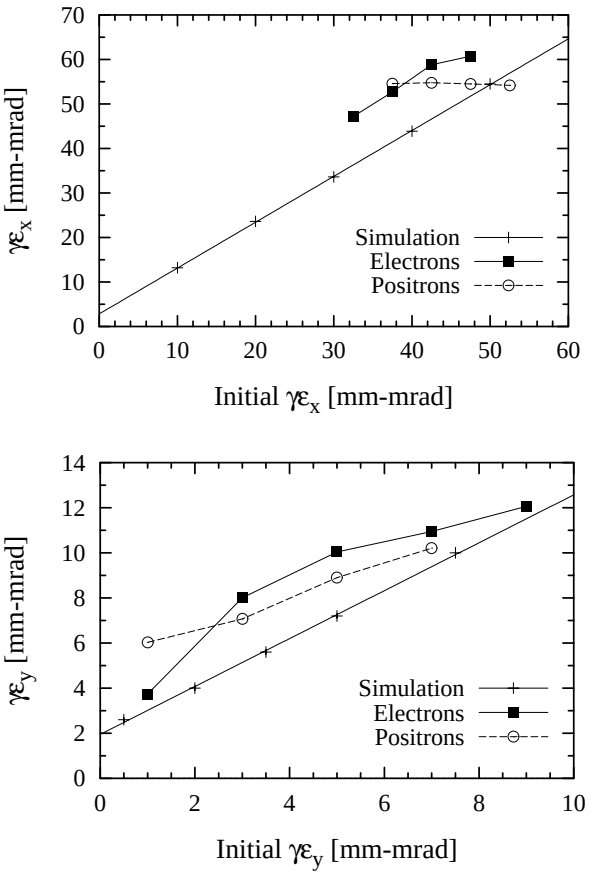

Figure 8 Normalized horizontal and vertical emittances at sector 28 against the initial values. Simulation results for electrons are compared to the electron and positron average performance during the 1996 run. Statistical errors are too small to be visible.

The simulation results can be parameterized in the form:

$$\gamma\varepsilon_{28} = \kappa \cdot \gamma\varepsilon_{initial} + \Delta\gamma\varepsilon_{wf} \qquad (3)$$

Multiplicative emittance growth is characterized by κ, while wakefield generated emittance growth is additive and is described by the term $\Delta\gamma\varepsilon_{wf}$. Fits to the simulation results provide:

- $\kappa = 1.03$, $\Delta\gamma\varepsilon_{wf} = 2.83$ (27) mm-mrad (electron X)
- $\kappa = 1.06$, $\Delta\gamma\varepsilon_{wf} = 1.95$ (21) mm-mrad (electron Y)

The simulated additive emittance growth without bump optimization is indicated in brackets. Multiplicative emittance growth is expected to be small. The measured 1996 emittances indeed do not provide any indication for large multiplicative emittance growth (larger than expected slope).

The measured growth $\Delta\gamma\varepsilon_{wf}$ is determined from the 1996 data for the average injected emittance:

- $\gamma\varepsilon_{initial} = (36.3 \pm 4.1)$ mm-mrad (electron X)
- $\gamma\varepsilon_{initial} = (5.0 \pm 1.5)$ mm-mrad (electron Y)
- $\gamma\varepsilon_{initial} = (44.0 \pm 3.9)$ mm-mrad (positron X)
- $\gamma\varepsilon_{initial} = (2.4 \pm 1.0)$ mm-mrad (positron Y)

The numbers indicate the 1996 average values and their standard deviations. With those injected emittances one obtains from Figure 9:

- $\Delta\gamma\varepsilon_{wf} \sim 13$ mm-mrad (electron X)
- $\Delta\gamma\varepsilon_{wf} \sim 5$ mm-mrad (electron Y)
- $\Delta\gamma\varepsilon_{wf} \sim 11$ mm-mrad (positron X)
- $\Delta\gamma\varepsilon_{wf} \sim 4$ mm-mrad (positron Y)

The average additive emittance growth in the SLAC linac is reduced by factors of more than 2 in x and more than 4 in y due to bumps. However, the emittance growth is still larger than the simulated performance by ~ 9 mm-mrad in x and ~ 2.5 mm-mrad in y. This discrepancy can be explained to a large extent by the tuning stability in the linac. Note, that the predicted performance was almost achieved for electrons with small incoming vertical emittances. Occasionally emittance growth as small as 1 mm-mrad was measured in the SLAC linac.

Tuning stability

Once the final beam emittance has been optimized in the SLAC linac, the trajectory looks similar to that shown in Figure 5. The trajectory and the phase relations of structure and quadrupole errors must be kept constant in order to maintain the optimized emittance. Any drift in the beam optics will cause additional wakefield emittance growth.

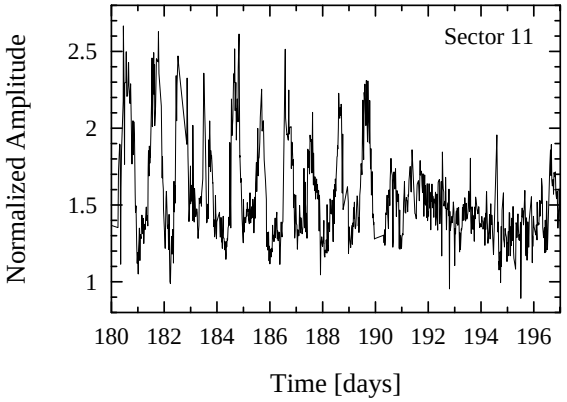

Figure 9 Variation of the normalized amplitude of a betatron oscillation in sector 11 of the SLAC linac. A fix was applied on day 191 [5].

The SLAC linac is subject to large day-night variations in the beam optics. The beam phase advance changes by up to 130º and the amplitude growth of an incoming betatron oscillation varies by factors of about 2. An example is shown in Figure 9 for the location between the two linac bumps. It is immediately clear that the bump optimization is heavily disturbed by those changes in the beam optics.

As day-night transitions occur every 12 hours and the bump optimization takes several hours itself, bumps are tuned constantly. The measured average emittance growth is significantly increased beyond the simulated value that assumes full optimization. The emittance sta-

bility can be quantified from the observed spread in emittance measurements (compare Figure 7). The spread in the final linac emittances agrees well for electrons and positrons and one obtains:

- σ_ε = 5.9 mm-mrad (x)
- σ_ε = 2.8 mm-mrad (y)

Correcting for the spread of the incoming emittances (see above) the emittance spread generated in the linac is calculated to be 4.5 mm-mrad in x and 2.4 mm-mrad in y. The larger spread in x may indicate less frequent tuning. The relative emittance increase (important for luminosity reduction) is smaller in x than in y. The difference $\Delta\varepsilon_{unexplained}$ between the measured average emittances in the linac and the predicted values can be expressed in terms of emittance stability:

- $\Delta\varepsilon_{unexplained} \sim 1.5\ \sigma_\varepsilon$ (x)
- $\Delta\varepsilon_{unexplained} \sim 1\ \sigma_\varepsilon$ (y)

It is not unreasonable to assume a 1 σ loss of emittance performance due to continual tuning of linac bumps and large day-night variations.

Pulse-to-pulse jitter

The typical SLAC linac trajectory looks similar to the one shown in Figure 6. It was already pointed out that wakefields change the beam optics. The phase advance and the normalized strength of a betatron oscillation are a function of the wakefield strength. Because the amplitude of wakefield deflections depends on the bunch length and current, any change in those parameters will change the beam optics and the beam trajectory. Incoming charge and current jitter translates into transverse position jitter. This was studied in [7].

If BNS damping is not fully implemented (as in the SLAC linac) a betatron oscillation will also cause emittance growth. It is important to note that transverse beam jitter translates into emittance jitter. The measured SLC beam emittance, measured over many hundred pulses, is increased. This effect must be studied further.

Limitations and alternatives

The present performance of the SLAC linac is limited by the stability of the beam optics. Long oscillation bumps are especially sensitive against optics changes. Several ideas have been proposed to determine the structure to beam offsets in the SLC and then to steer the beam through structure centers [8,9,10]. No bumps would be needed and errors are corrected on a local scale.

In order to evaluate this approach we consider the expected emittance without wakefields and without bumps. Simulations predict a dispersive emittance growth of 5.1 mm-mrad in x and 3.9 mm-mrad in y. This must be compared to the measured average emittances during the 1996 run: 12 mm-mrad in x and 4.5 mm-mrad in y. Perfect elimination of wakefield deflections in y will bring only a slight improvement, if dispersion remains uncorrected. Steering through the structure centers will even increase the RMS beam to quadrupole offset and therefore the expected dispersive emittance growth.

6 SUMMARY

Multi-particle beam dynamics in the SLC linac was discussed with an emphasis on the emittance transport. The emittance optimization, done with linac bumps, was shown to work very well. Wakefield generated and dispersive emittance growths are optimized simultaneously.

The emittance performance during the 1996 run was shown to agree within 1-1.5 standard deviations of its measured variation with simulations. The average performance was limited by the tuning stability of the linac. Occasionally emittance growth as small as 1 mm-mrad was measured in the vertical plane. Though the large horizontal emittances are suspicious, the data does not indicate larger than expected multiplicative emittance growth.

New optimization methods, that avoid the usage of bumps, will only then significantly improve the emittance performance, if dipole wakefields and dispersion are optimized simultaneously.

7 ACKNOWLEDGEMENTS

I wish to thank R. Siemann for his active interest and support. I further thank C. Adolphsen, K. Bane, A. Chao, F.J. Decker, N. Phinney, P. Raimondi, T. Raubenheimer, M. Ross, W. Spence, G. Stupakov and F. Zimmermann for many stimulating discussions.

REFERENCES

[1] K. Bane and P. Wilson. Proc. 11th Int. Conf. On High Energy Accelerators, CERN 1980, p.592.
[2] R. Assmann et al, “LIAR - A computer program for the modeling and simulation of high performance linacs”. SLAC/AP-103.
[3] F.J. Decker et al., “Long-range wakefields and split-tune lattice at the SLC”. SLAC-PUB-7259 (1996).
[4] R.H. Holtzapple. Stanford University, PhD Thesis 1996.
[5] R. Assmann et al, “Monitoring of the SLC optics with a diagnostic pulse”. These proceedings.
[6] J. Seeman et al, “The introduction of trajectory oscillations to reduce emittance growth in the SLC linac”. SLAC-PUB-5705 (1992).
[7] C. Adolphsen et al, “Beam Trajectory Jitter in the SLC Linac”. PAC95.
[8] R. Assmann et al, “Observation and Analysis of Static Deflections from Transverse Long-Range Wakefields in the SLC”. These proceedings.
[9] F.J. Decker et al, “Super-ASSET: A Technique for Measuring and Correcting Accelerator Structure Misalignments at the SLC.”. These proceedings.
[10] M. Seidel et al, “Detection of Beam-Induced Dipole-Mode Signals in the SLC S-Band Structures”. These proceedings.